Geomechanics and Engineering, *Vol. 31, No. 2 (2022) 183-195*
https://doi.org/10.12989/gae.2022.31.2.183

Seismic behavior of the shallow clayey basins subjected to obliquely incident wave

Hadi Khanbabazadeh*[1], Recep Iyisan[2a] and Bilal Ozaslan[2b]

[1]*Department of Engineering Gebze Technical University, Kocaeli, Turkey*
[2]*Department of Civil Engineering, Istanbul Technical University, Istanbul, Turkey*

(*Received January 1, 2021, Revised July 19, 2022, Accepted October 12, 2022*)

Abstract. Under the effects of the near-field earthquakes, the incident angle of the incoming wave could be different. In this study, the influences of some parameters such as incident angle, basin edge, peak ground acceleration level of the bedrock motion as well as different clay types with different consistency on the amplification behavior of the shallow basins are investigated. To attain this goal, the numerical analyses of the basins filled with three different clay types are performed using a fully nonlinear method. The two dimensional models of the basins are subjected to a set of strong ground motions with different peak ground acceleration levels and three different incident angles of 30◦, 45◦ and 90◦ with respect to the horizontal axes. The results show the dominant effect of the obliquely subjected waves at most cases. The higher effect of the 45◦ incident angle on the basin response was concluded. In the other part of this study, the spectral amplification curves of the surface points were compared. It was seen that the maximum spectral amplification of different surface points occurs at different periods. Also, it is affected by the increase in the peak acceleration level of the incoming motions.

Keywords: basin edge effect; dynamic behavior; incident angle; numerical modeling; site effects

1. Introduction

The fact that the seismic motion recorded at the ground surface is affected by irregular basin stratification and geometry is known as site effect. It is done by focusing, defocusing, diffraction and scattering of seismic waves. In this way, specifications of the bedrock motion such as amplitude, frequency content and duration are affected compared to stiff and flat ground conditions (Safak 2001, Assimaki and Gazetas 2004, Pelekis *et al.* 2017, Zhu *et al.* 2018, Khanbabazadeh *et al.* 2020). Also, the incident angle of the incoming waves and conversion of the body waves to surface waves are among other factors influencing the dynamic response of the sites (Heymsfield 2000, Takahiro 2000, Gil-Zepeda *et al.* 2003, Zhu and Thambiratnam 2016). Assessment of the amplification factor is a way to investigate the site effect (Anbazhagan *et al.* 2011, Jakka *et al.* 2015, Shiuly *et al.* 2015, Gautam *et al.* 2016, Khanbabazadeh *et al.* 2018, Costanzo *et al.* 2019). In practice, the term site amplification is used to represent any differences in ground motions between two nearby sites.

This effect could be inferred using 1D models. Nevertheless, several field investigations showed the insufficiency of the approaches based on 1D site response (Roy and Sahu2012, Iyisan and Khanbabazadeh 2013, Madiai *et al.* 2016, Abraham *et al.* 2015, Sonmezer *et al.* 2018, Sonmezer and Celiker 2020). The seen higher damage pattern at the edge of the shallow basins with respect to the central parts aroused the ideas of the effect of the inclined bedrock on basin behavior. The concentration of the damages at the edge of Dinar basin (Bakir *et al.* 2002, Khanbabazadeh *et al.* 2016) and Duzce basin in Turkey (Khanbabazadeh *et al.* 2019, Hasal *et al.* 2018), Volvi Basin in Greece (Raptakis *et al.* 2000, Pitilakis 2004) Miyagi and Fukushima in Japan (Kamiyama and Satoh 2002) and Euroseistest site (Makra *et al.* 2005) provided more accurate data about the basin edge effect. The investigation of the lateral heterogeneity, focusing and locally generated surface waves effects gained popularity among researchers (Makra and Chavez-Garci 2016, Yniesta *et al.* 2017, Stanko *et al.* 2019).

After the pioneering semi-analytical/semi-numerical work of Aki and Larner (1970) several analytical and numerical methods have been applied in the investigation of the different aspects of the site effect (Paolucci 1999, Faccioli *et al.* 2002, Rodriguez-Castellanos *et al.* 2011, Kham *et al.* 2013). Finite element and finite difference methods, boundary element method (direct and indirect) and hybrid techniques are among the most used techniques (Chavez-Garcia *et al.* 2000, Kamalian *et al.* 2006, Zhang and Zhao 2009, Gelagoti *et al.* 2010, Shani-Kadmiel *et al.* 2012, Saffarian and. Bagheripour 2014). Despite the development of the robust numerical methods, because of the difficulty of the application of 2D and 3D analyses, some attempts were made to make correlation between 1D and 2D results. Nevertheless, in most of the cases, the application of 2D and 3D analyses for basins with irregular

*Corresponding author, Assistant Professor
E-mail: hk.babazadeh@gtu.edu.tr
[a]Professor
E-mail: iyisan@itu.edu.tr
[b]Professor
E-mail: ozaslanb@itu.edu.tr

ISSN: 2005-307X (Print), 2092-6219 (Online)

Table 1 The geotechnical properties of the considered three clay types

Soil classification		c (kPa)	ϕ (°)	V_s (m/s)	G (kPa)	K (kPa)	γ (kN/m^3)	PI (%)
Clay	Stiff	150~165	10	450~650	4e5~9e5	10.6e5~23.7e5	20~21.5	55
	Medium	75~90	10	200~400	0.76e5~3.36e5	2e5~8.8e5	19~21	30
	Soft	35~45	10	75~175	10.1e3~61.2e3	26.4e3~159.7e3	18~20	10
Bedrock	Elastic	-	-	1000	22e5	36e5-	22	-

ϕ: internal friction angle; c: cohesion; V_s: shear wave velocity; G: shear modulus;
K: bulk modulus; γ: unit weight

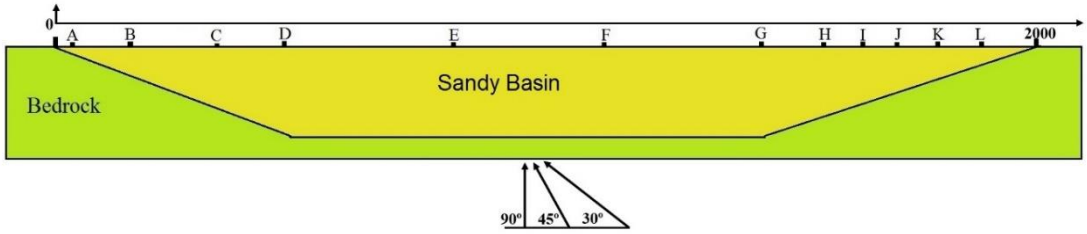

Fig. 1 The geometry of the considered clayey basins for (a) vertical and (b) obliquely incident wave

geometries are inevitable (Semblat *et al.* 2005, Manakou *et al.* 2010, Khanbabazadeh and Iyisan 2014a, b, Saenz *et al.* 2019).

The common method in modeling wave transmission in layered sites and dynamic soil-structure interaction in geotechnical earthquake engineering is the equivalent linear method. The application of this scheme yields suitable results in medium strain range. However, by the increase in strains to large strain level, the application of the fully nonlinear method becomes inevitable. This method follows any prescribed nonlinear constitutive relation. Also, both shear and compressional waves are propagated together in a single simulation, and the material responds to the combined effect of both components.

In most of the studies, the dynamic response of the basins is studied under the effect of the vertically propagating waves. The influence of obliquely incident wave can be more important for shallow basins under the effect of near field earthquakes. In such case, the dynamic response of a symmetric basin at two edges would be different (You *et al.* 2009, Zhu *et al.* 2015). The main purpose of the present study is to investigate the dynamic response of the shallow clayey basins under the effect of different incident angles. Also, the effect of some parameters such as basin edge, bedrock PGA level as well as different clay types on the amplification behavior of the basins are investigated. To get more realistic results under the effect of the strong ground motions, the dynamic analyses are performed in time domain using a fully nonlinear method which utilizes explicit finite difference scheme (Cundall 2008). In this way, in addition to its advantage in the modeling of 2D geometries, the interference and mixing of different frequency components occur naturally.

The mesh generation and modeling procedure of the obliquely propagating waves in FLAC is different from the modeling of the vertically propagating waves. It is mainly related to the application conditions of the free-field dynamic boundary condition. The modeling of the incident angles other than vertical cases has been done with respect to the special instruction presented by Cundall (2008) in FLAC3D manual for such cases. Also, based on Kuhlemeyer and Lysmer (1973), the spatial element size was selected smaller than one eighth of the wavelength associated with the highest frequency component of the used motions. In order to completely catch basin edge effect, the basin width has been taken too long (2000 m) so that these effects are caught. If the results show the influence of inclined bedrock at beyond the basin edge, the width can be increased. The analyses results have shown the sufficiency of the selected width to depth ratio for these set of analyses. In Fig. 1, the geometry of the representative shallow sandy basin, the incident wave angles as well as the location of the recording points along the basin surface are presented. The variation of the response under applied motions has been recorded at 12 points over the basin surface.

2.2 Analysis method

A fully nonlinear method based on finite difference scheme which uses explicit finite difference scheme to solve the full equations of motion in time domain has been utilized in this research. This type of analysis is done using FLAC code (Fast Lagrangian Analysis of Continua). In this method, the first-order space and time derivatives of a variable are approximated by finite differences, assuming linear variations of the variable over finite space and time intervals, respectively. Then, the continuous medium is

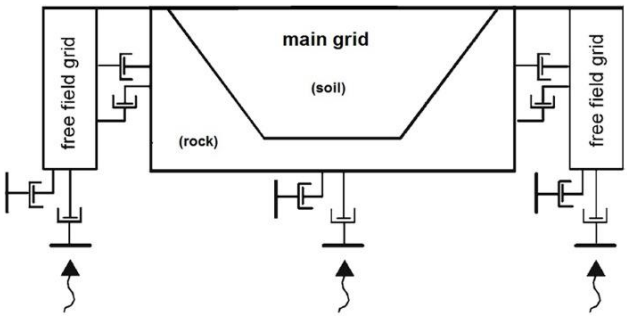

Fig. 2 The schematic coupling of the main grid to quiet boundary and free-field grids

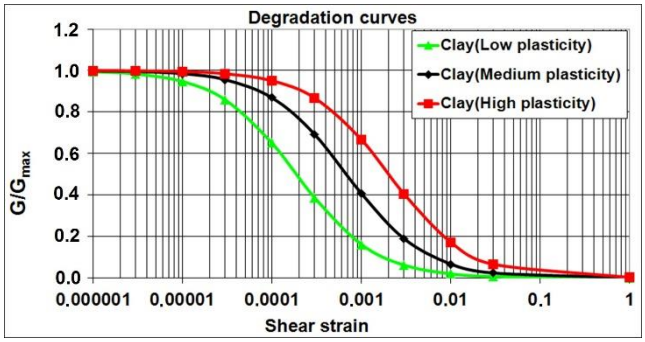

Fig. 3 The corresponding degradation curves for selected clay types

replaced by a discrete equivalent one in which all forces involved (applied and interactive) are concentrated at the nodes of a mesh used in the medium representation. Finally, the inertial terms in the equations of motion are used as numerical means to reach the equilibrium state of the system under consideration.

2.2.1 Boundary conditions

The flexible base boundary condition has been used in the bottom of the models. In this case, the quiet boundary scheme proposed by Lysmer and Kuhlemeyer (1969), which involves dashpots, is attached independently to the horizontal boundary in the normal and shear directions. In effect, by preventing the reflection of outward propagating waves back into the model, the radiation of energy is provided.

Also, free-field boundary condition is used for the vertical boundaries at the model sides. In this approach, based on method used in NESSI (Cundall 1980), the free-field calculations are executed in parallel with the main-grid analysis. In Fig. 2 the schematic coupling of the main grid to quiet boundary and free-field grids is presented.

2.2.2 Damping and degradation curves

The combination of the Hardin/Drnevich hysteretic damping with a Mohr–Coulomb model is utilized. The hysteresis damping scheme incorporates strain dependent damping ratio and secant modulus functions. It is applied by modifying the strain rate calculation so that the mean strain-rate tensor (averaged over all subzones) is calculated before any calls are made to constitutive model functions. At the meantime, the application of the fully nonlinear method provides possibility so that a hysteretic-type model is incorporated with no extra damping specification. It is done by introducing only degradation curves in the form of special fitted functions. Then, by the application of the Hardin/Drnevich model, the corresponding damping with respect to the level of excitation at each point in time and space are calculated. In this way, the modulus reduction technique is applied in the elastoplastic range, while natural damping is applied in the plastic range. The corresponding degradation curves for selected clay types have been obtained using the relations presented by Ishibashi and Zhang (1993) and are shown in Fig. 3. The fitting operation of these curves to FLAC code has been fulfilled using a fish which determines the coefficients of the built-in function corresponding to the used degradation curves.

2.3 Strong ground motions

The two dimensional models of the clayey basins are subjected to a set of strong ground motions with three different incident angles. The considered incident angles are 30◦, 45◦ and 90◦ with respect to the horizontal axes. The used motion set comprises sixteen earthquakes with four PGA levels of 0.1 g, 0.2 g, 0.3 g and 0.4 g; four motions for each PGA level. The incident waves are of SV type, and have been produced by the similar faulting mechanism (right strike-slip). Also, to remove the effect of soil layers from selected accelerograms, they have been chosen from motions recorded on stiff soils during real earthquakes, or deconvoluted to the corresponding bedrock motion. These records are of different PGAs, frequency contents and durations. All of them have been baseline corrected and filtered with a 25 Hz low-pass filter. In Table 2 the specifications of the used earthquakes are presented.

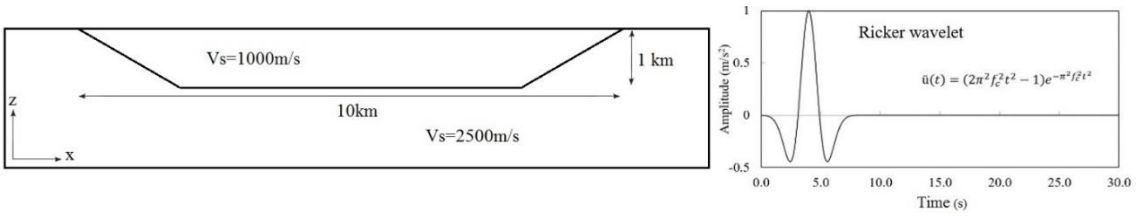

Fig. 4 Geometry of the verification model and the used bedrock motion

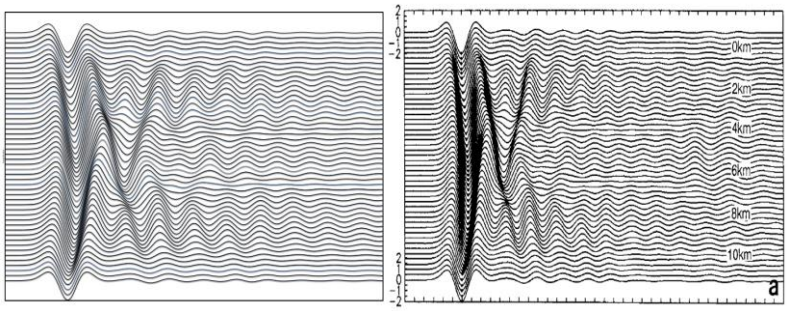

Fig. 5 Comparison of the results between the verification model and the method used in this study

Table 2 The specifications of the used strong ground motions

	Earthquakes	Station	Amax (g)	Magnitude	R_{JB}	Arias Intensity (m/s)
1	Mammoth lakes (25.05.1980)	USC McGee Creek	0.1	Mw=6.0	7	0.1
2	Anza (25.02.1980)	PinyonFlat	0.1	Mw=5.19	12	0.022
3	Palm springs1986	Silent Valley	0.1	ML=5.9	20	0.1
4	Chalfant (21.07.1986)	LongValleyDam	0.1	Mw=6.2	15	0.2
5	Sakarya (11.11.1999)	Development burea	0.2	Md=5.7	18	0.14
6	Dinar (01.10.1995)	Dinar station	0.2	ML=5	2	0.81
7	Duzce (12.11.1999)	Lamont-531	0.2	Mw=7.1	11	0.528
8	Livermore (27.01.1980)	Morgan Terr Park	0.2	Mw=5.4	10	0.188
9	Mendocino 1992	EEL River valley	0.3	ML=6.5	15	0.808
10	Coyotelake (06.08.1979)	Coyote Lake Dam	0.3	Mw=5.7	2	0.4
11	Parkfield (28.06.1966)	Temblor pre	0.3	Mw=6.1	16	0.362
12	Firuzabad 20.06.1994	Firuzabad-ZRT	0.3	Mw=5.9	21	0.687
13	Kocaeli1(07.08.1999)	Development burea	0.4	Md=7.4	4	1.584
14	Parkfield (28.06.1996)	Temblorpre	0.4	Mw=6.1	16	0.554
15	UmbriaMarche (10.16.1997)	Colfiorito-Casermette	0.4	Mw=4.3	1	0.69
16	South Iceland (17.06.2000)	Thjorsarbru	0.4	Mw=6.5	15	1.613

2.4 Verification

In this section the verification of the applied numerical modeling is presented. To do that, the 2D solution of the trapezoidal valley estimated by Kawase and Aki (1989) and tested by Zahradnik (1995), Gil- Zepeda *et al*. (2003) and Zhu and Thambiratnam (2016), among others, is used. In Fig. 4, the geometry of the basin and the applied Ricker pulse as the bedrock motion are shown.

The comparison of the results between the method used in this study and the verification model has been presented in Fig. 5. The estimated results are fairly close.

3. Results and discussion

3.1 Variation of the Maximum Spectral Amplification Factor (MSAF)

In this study, the acceleration time histories under the effect of applied each motion were recorded at 12 surface points in time domain. The horizontal component of the surface motion (the component along the basin surface direction) has been obtained and used. For all incident angles, the spectral amplification has been estimated with respect to the corresponding free-field condition. The

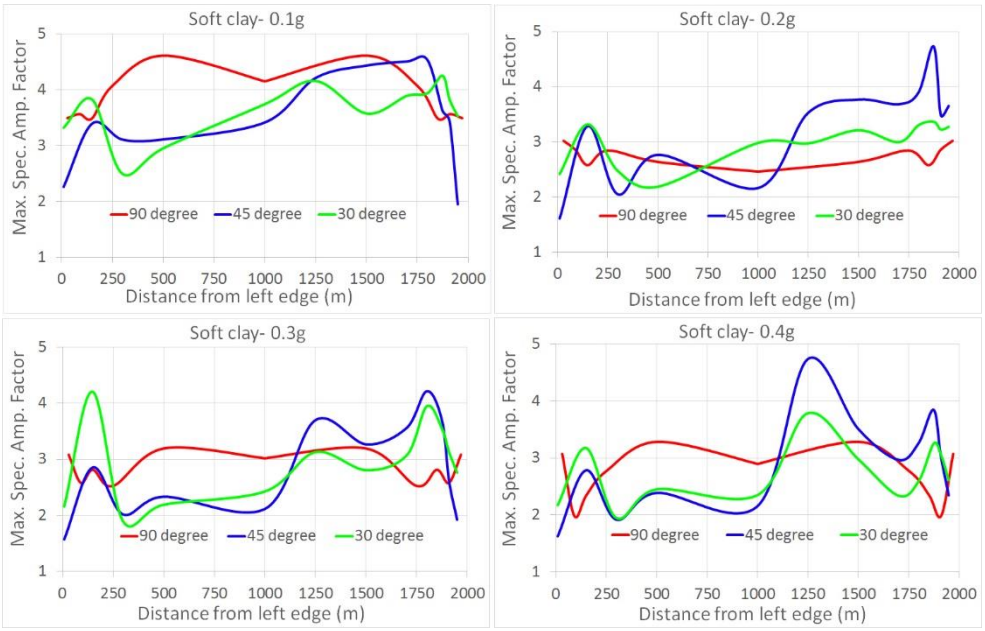

Fig. 6 The variation of the MSAF over soft clayey basin surface

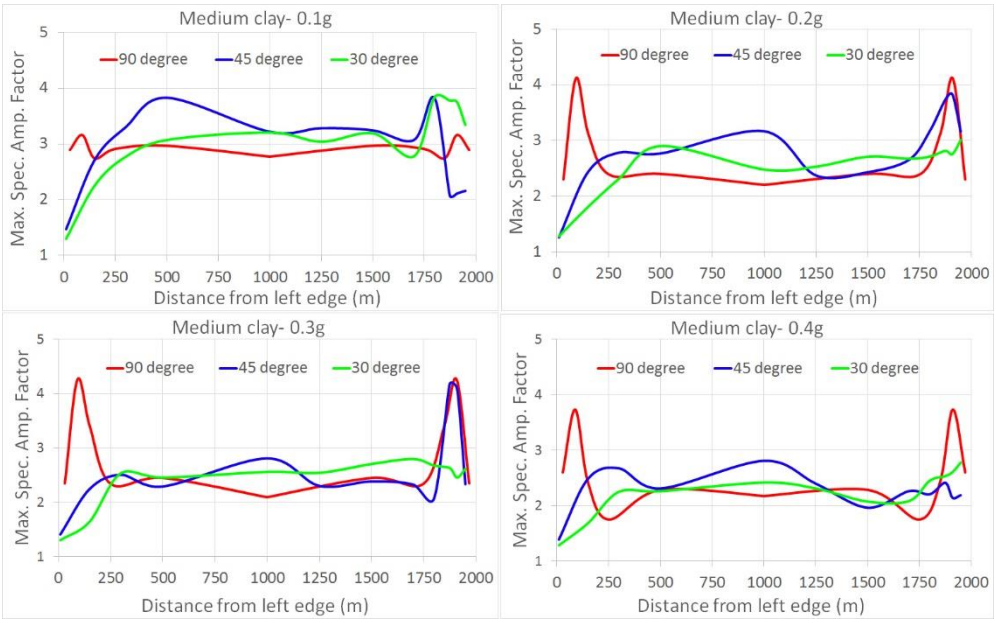

Fig. 7 The variation of the MSAF over medium plasticity clayey basin surface

spectral amplification is defined as the ratio of the spectral acceleration at each point on the basin to the free-field (rock outcrop). Then, the average of the spectral amplification curves under four earthquakes with the same PGA level was estimated and reported. The influences of some parameters such as basin edge, PGA level of the bedrock motion and incident angle as well as different clay types on the amplification behavior of the basin are discussed.

3.1.1 Soft clayey basin

Fig. 6 shows the variation of the MSAF over soft clayey basin surface for different PGA levels. It is seen that, except at the edges, under the effect of motions with PGA of 0.1 g the MSAF of the 90◦ incident angle is dominant. By the increase in the PGA level to 0.2 g, the effect of 45◦incident angle becomes dominant at eastern half. The response of the western half is almost close for 30◦ and 45◦ incident angles. In this case, the difference between MSAF at eastern and western edges (4.8 and 3.2, respectively) is noticeable.

For motions with PGA level of 0.3 g, although the effect of 45◦ incident angle is still dominant at eastern half, the effect of 30◦ incident angle becomes dominant at western edge. At the large part of the western half the effect of 90◦ incident angle is dominant. In this case, despite almost similar MSAFs at the edges, they correspond to different incident angles. The dynamic response of this basin under the effect of motions with PGA level of 0.4 g becomes different with respect to weaker motions. In this case, in

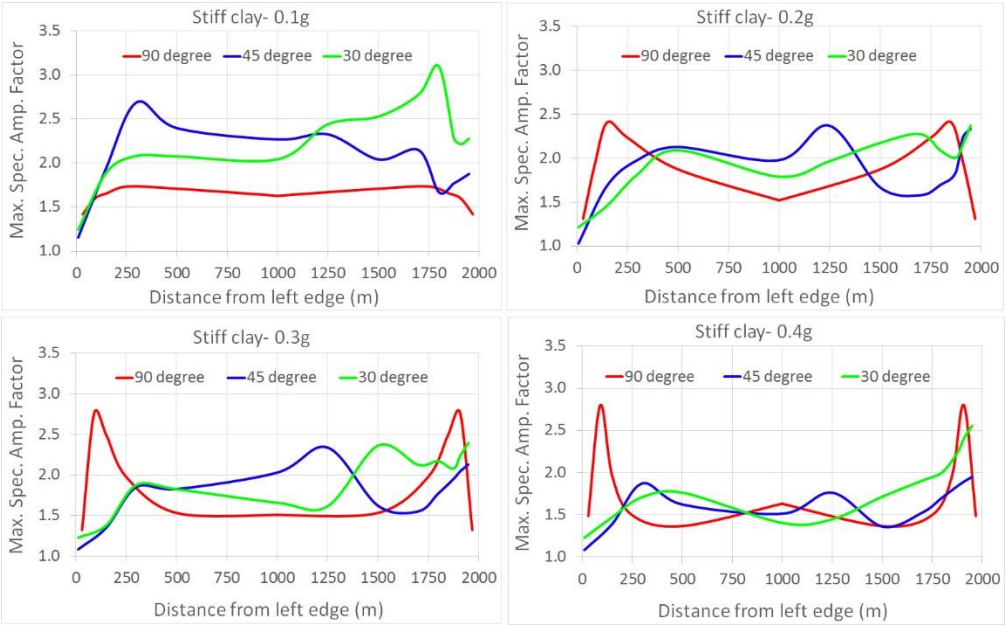

Fig. 8 The variation of the MSAF over stiff clayey basin surface

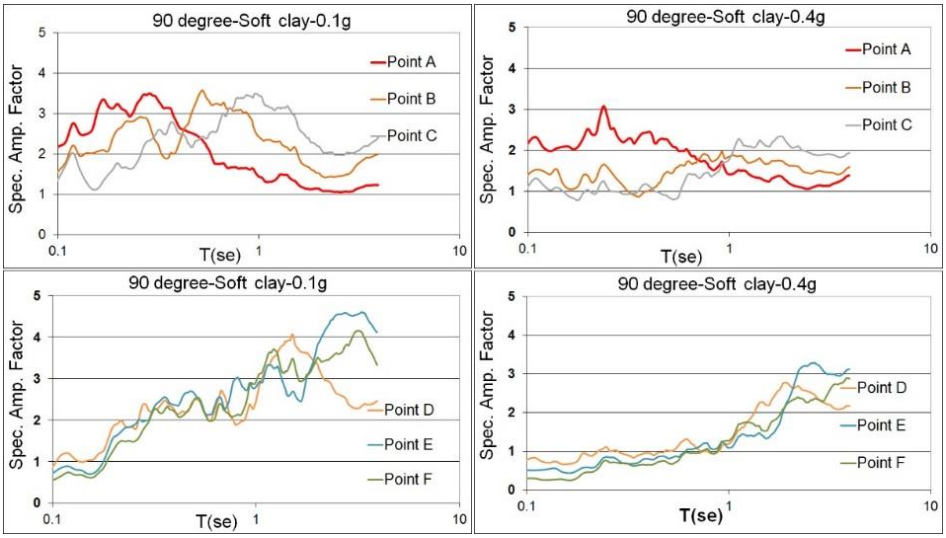

Fig. 9 The SAF curves of the soft clayey basin surface (incident angle: 90◦).

addition to the asymmetric response of the basin, the location of the peak moves to the region outside the basin edge. Both of these peaks belong to the 45◦ incident angle.

3.1.2 Medium plasticity clayey basin

The analysis results of the medium plasticity clayey basin presented in Fig. 7 show that for motions with PGA level of 0.1 g, the MSAFs decreases (about 3.8) with respect to the soft clayey basin (about 4.7). For motions with PGA level of 0.2 g the effect of 90◦ incident angle becomes dominant at both edges. Almost similar trend is seen for medium clayey basin for motions with PGA level of 0.3 g. By the increase in PGA level to 0.4g, while the effect of the 90◦ incident angle is dominant at both edges, the effect of the 30◦ incident angle is dominant at central parts. For this case, the estimated MSAFs are smaller with respect to the soft clayey basin.

3.1.3 Stiff clayey basin

In Fig. 8 the dynamic response of the basin filled with the stiffest clay type of this study is presented. Under the effect of the motions with lower PGA level (0.1 g), the higher effect of the 30◦ incident angle at the eastern half of the basin is noticeable.

In the meantime, the effect of 45◦ incident angle is dominant at the western half. By the increase in PGA level to 0.2 g, the effect of the 90◦ incident angle becomes dominant at edges while the MSAFs at almost whole of the central part occurs at 45◦ incident angle. Almost similar trend but with different MSAF is seen for motions with PGA of 0.3 g. Regarding the motions with PGA of 0.4 g, while the change in incident angle doesn't significantly affect the response at central part, the highest MSAFs occur at the basin edges under the effect of 90◦incident angle.

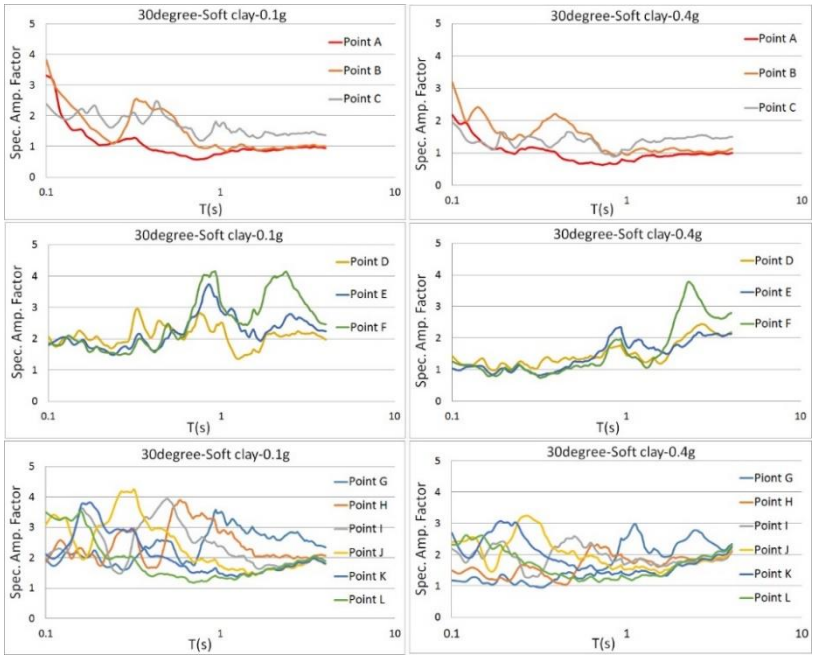

Fig. 10 The SAF curves of the soft clayey basin surface (incident angle: 30◦).

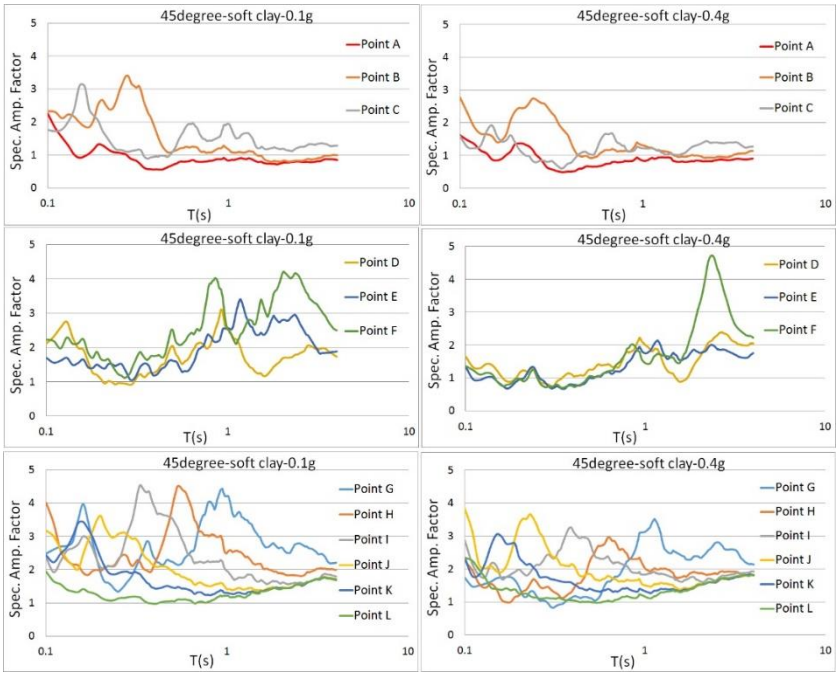

Fig. 11 The SAF curves of the soft clayey basin surface (incident angle: 45◦)

3.2 Spectral amplification factor (SAF) curves

The presented results in Fig. 6-8 show only the variation of the MASFs over basin surface, and give no information about their period. To see the change in their corresponding period, the spectral amplification curves of the surface points are compared in this section. The comparison is done between just the estimated responses under the effect of the motions with PGA of 0.1 g and 0.4 g. Also, for explanation purposes, the basin surface is divided into three regions. These regions will be referred as far edge (about 300 meters from western outcrop including points A, B and C), central part (about 1200 meters including points D, E and F) and near edge (about 500 meters from eastern outcrop including points G, H, I, J, K and L).

3.2.1 Soft clayey basin

Fig. 9 presents the SAF curves of the different points at soft clayey basin surface for vertically propagation of the shear waves. For this case, because of the symmetric behavior of the basin, just the curves of the half of basin are presented. The results show that, under the effect of the

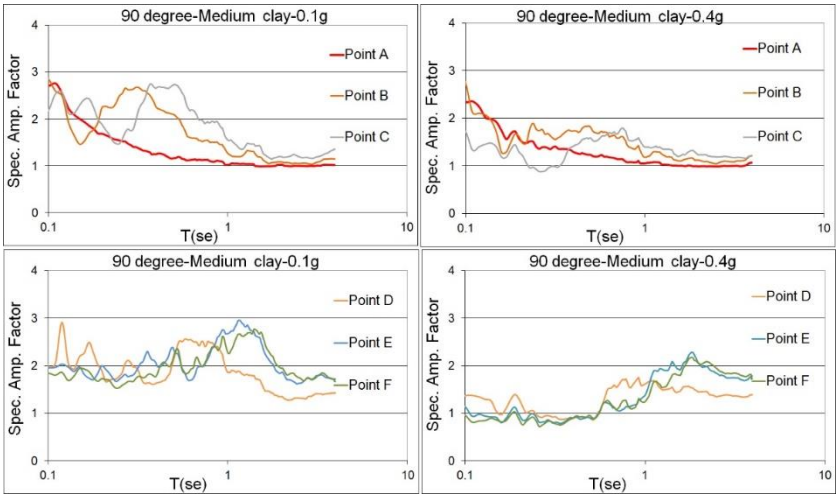

Fig. 12 The SAF curves of the medium clayey basin surface (incident angle: 90◦)

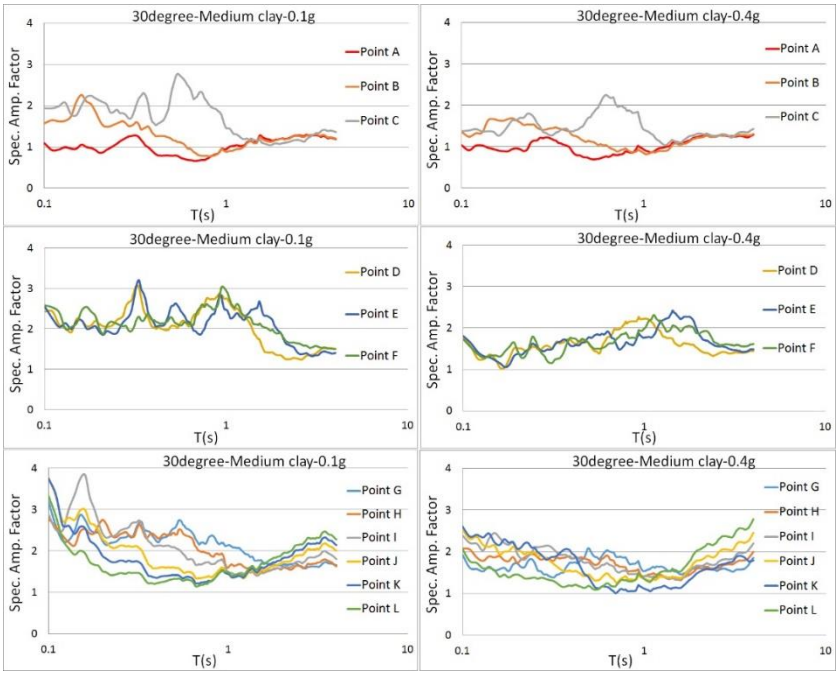

Fig. 13 The SAF curves of the medium clayey basin surface (incident angle: 30◦)

motions with PGA of 0.1 g, period of the MSAF of points A, B and C increases by the increase in the distance from outcrop. From point D on, all curves converge to almost one curve, which indicates the cancellation of the basin edge effect and uniform behavior along this region. Also, by the increase in motion PGA level, a slight increase in period of the MSAFs occur. It can be concluded that while the MSAF of the points close to the outcrop occur at lower period, the MASF of the farther points occur at periods greater than 1.

For incident angle of 30◦ (Fig. 10) and PGA level of 0.1 g, while the MSAF of the points at far edge generally occurs at periods less than 0.5s, by the increase in the distance from outcrop it moves to periods greater than 0.9s at central part.

In the near edge, the scattering of the SAF curves increases with respect to the far edge (shows the non-uniformity of the behavior at this region). In this case, the period of the MSAFs decrease from about 0.8s at point H to about 0.15s at point L. Almost similar overall trend is seen for the curves of the motion with PGA level of 0.4g at central part but with different MSAF values.

For the incident angle of 45◦ (Fig. 11) and PGA level of 0.1 g, the results show a slight decrease in the period of the MSAF of the points at far edge with respect to the 30◦ incident angle. The high scattering in the SAF curves at near edge is seen in this incident angle. Also, the increase in the PGA level of the motions to 0.4 g causes a slight increase in the period of the MSAF at near edge with respect to PGA level of 0.1 g.

3.2.2 Medium plasticity clayey basin

Fig. 12 presents the SAF curves of the medium

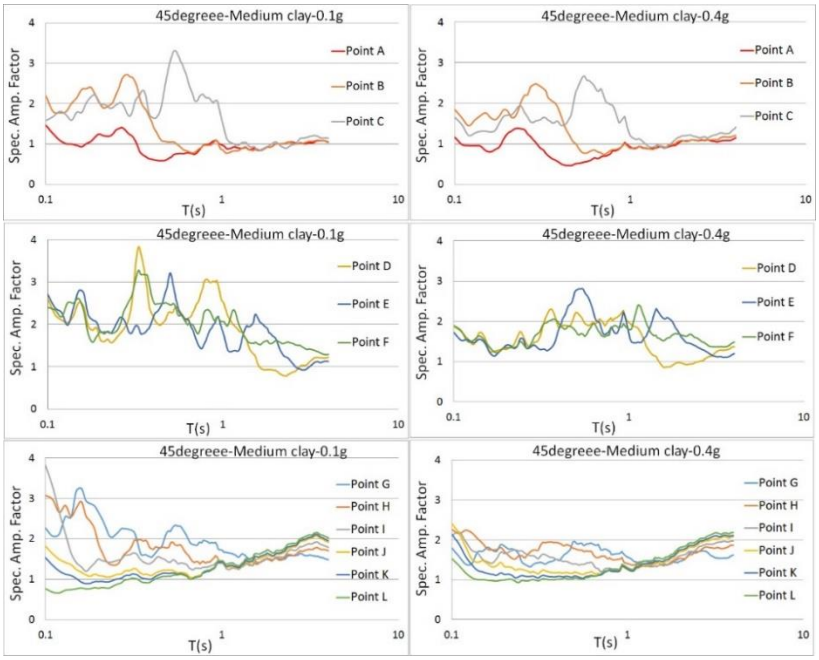

Fig. 14 The SAF curves of the medium clayey basin surface (incident angle: 45◦)

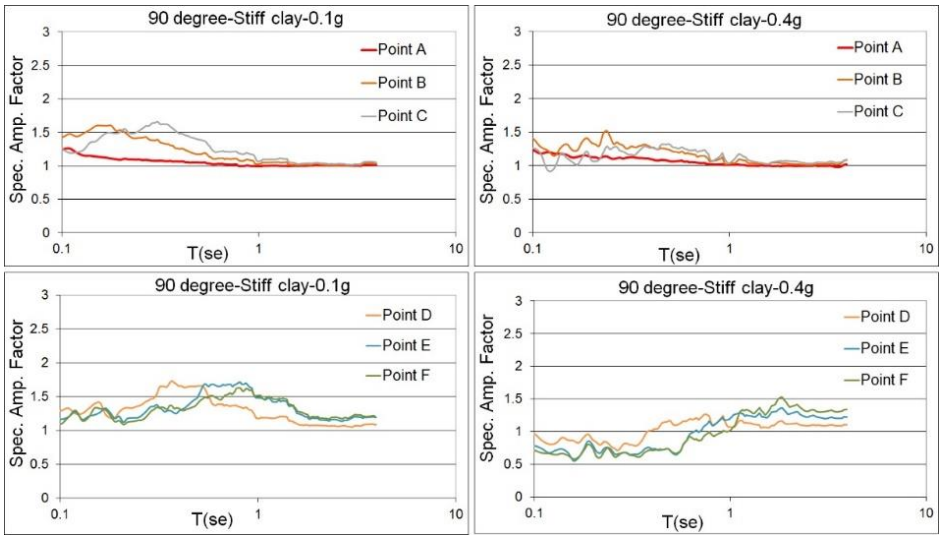

Fig. 15 The SAF curves of the stiff clayey basin surface (incident angle: 90◦)

plasticity clayey basin under the effect of the vertically propagating waves. There is a decrease in the period of the MSAFs at basin edge (PGA of 0.1 g) with respect to the soft clayey basin edge. Similar to the soft clayey basin, the sensitivity of the edge of this basin to lower periods can be seen. A slight increase in the period of the MSAFs can be seen by the increase in the PGA level of the motions. Also, the difference between the SAF curve of the point D and other points in central part of the basin indicate the longer influence of the basin edge in the case of the medium clayey basin.

For incident angle of 30◦ (Fig. 13), at the far edge the behavior of the point C becomes different from points A and B. Its MSAF occurs at higher period, and by the increase in the PGA level to 0.4 g increases slightly. At the central part, although the SAF curves converge to almost one curve for both PGA levels, the period of the MSAFs for PGA of 0.4 g reaches to above 1s. The scattering of the SAF curves at near edge increases with respect to the far edge. For this case, by the increase in the PGA level, the deviation of the SAF curves decreases.

By the increase in the incident angle to 45◦ (Fig. 14), the difference among SAF curves of the surface points at far edge increases. Also, the scattering in the SAF curves of the central part increases with respect to 30◦ incident angle.

No considerable change occurs in the period of the MSAFs by the increase in PGA level to 0.4 g. At the near edge, except the different behavior of the points G and H, the SAF curves of the other points are close to each other (decrease in the non-uniformity of the behavior in this region). The scattering at the near edge decreases by the increase in PGA level to 0.4 g.

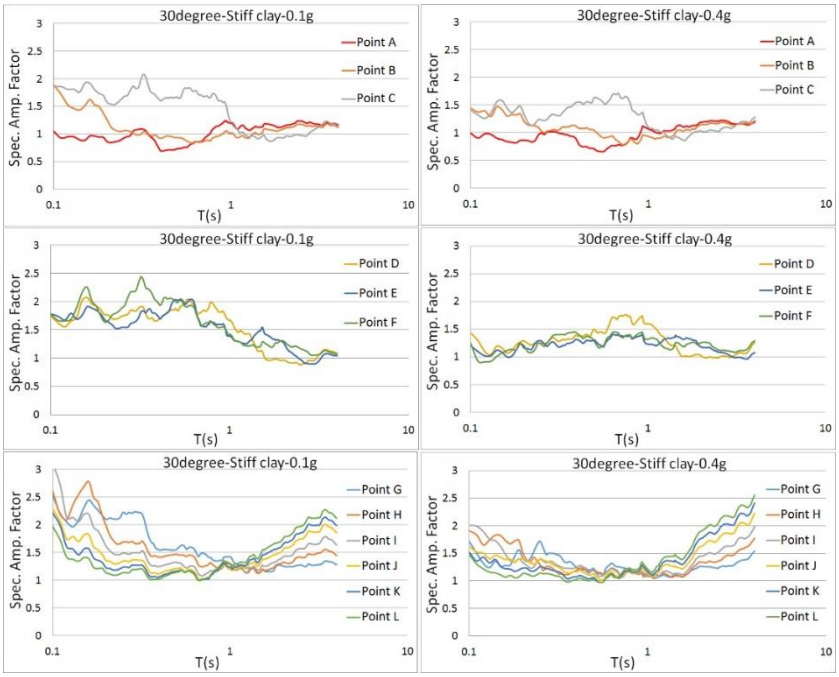

Fig. 16 The SAF curves of the stiff clayey basin surface (incident angle: 30◦)

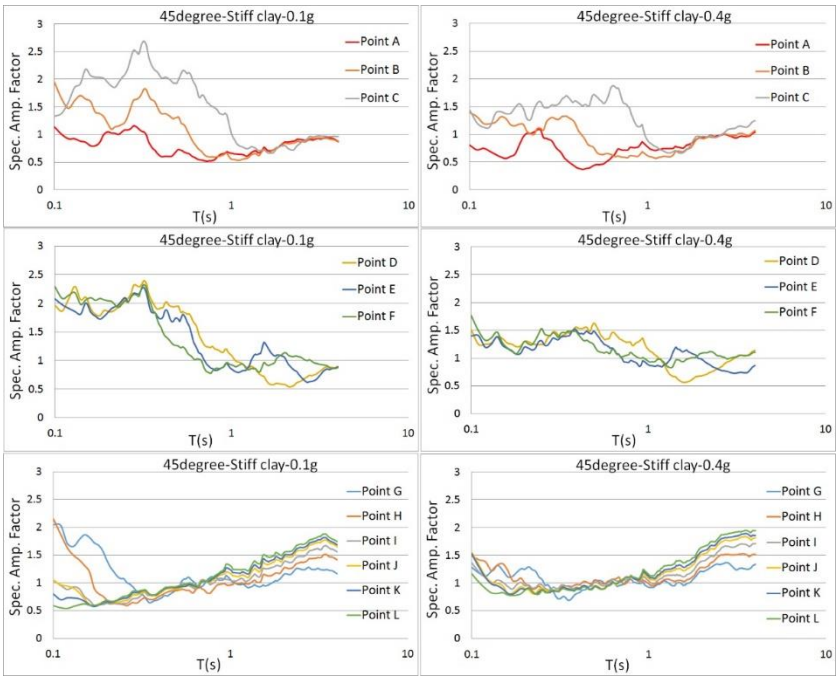

Fig. 17 The SAF curves of the stiff clayey basin surface (incident angle: 45◦)

3.2.3 Stiff clayey basin

In the case of the vertically propagating waves in stiff clayey basin (Fig. 15), the scattering of the SAF curves decreases at all points and PGA levels with respect to other clay types. Also, the period of the MSAFs under the effect of weaker motions at all edge and central points is less than other clayey basins. While the period of the MSAFs of the central points under the effect of weaker motions is less than 1s, it increases to greater than 1s for motions with PGA of 0.4 g.

For incident angle of 30◦ (Fig. 16), the behavior of the point C becomes more similar to the behavior of central part for both PGA levels. Despite the uniform behavior of the central part points under the effect of the both PGA levels, the period of the MSAF increases by the increase in the motion PGA level. In the near edge, two distinct peak points emerge in the SAF curves. These two peaks have periods less and greater than 1s. The uniformity of the response at near edge increases by the increase in PGA level to 0.4 g.

At the far edge of the stiff clayey basin and in 45◦incident angle (Fig. 17), the behavior of the points B and C become more similar to the behavior of central part points for both PGA levels. This indicate the higher effect of the 45◦incident angle on the behavior of the far edge. The closeness of the SAF curves at central part shows the uniform behavior under the effect of the both PGA levels. Nevertheless, by the increase in the PGA level the period of the MSAFs increases. At the near edge (0.1 g motions), except the point G and H with two distinct peak points, the period of MSAFs occur at period greater than 1s. By the increase in PGA level to 0.4 g, the SAF curves of the near edge turn to almost one curve with period of MSAF generally greater than 1s.

4. Comments on the wave propagation mechanics

In case of the vertically propagating waves, the interaction among the refracted waves, inclined bedrock and the generated surface waves give rise to a complicated situation. Several studies revealed that the dynamic response of shallow basins is generally dominated by the progress of the surface waves. Nevertheless, it should be noted that the existence of the surface wave doesn't necessarily mean the greater amplification. The interaction between the surface wave with other waves will determine the amplification or de-amplification at each single surface point. In an overall view, while the greater MSAFs have occurred in the middle parts of the softer basins, they have happened at the parts closer to the outcrop for stiffer basins. Also, if the width of the basin is taken long enough, the 1D behavior (corresponding to vertical wave propagation in a horizontal layering) at central parts can be seen.

The influence of obliquely incident wave can be more important for shallow basins under the effect of near field earthquakes. In this case, the symmetric behavior of the basin becomes asymmetric. Assuming the wave incidence from the east, the eastern inclined bedrock will refract the waves towards the inner parts of the basin. Besides, there will be an inclination in the direction of the waves enter from the basin bottom. In this case, there will be a wave flow towards the western edge of the basin. It will lead to a more complicated condition with respect to the vertical incident case. The seen behavior changes by the change in the soil type. In an overall view, the basins composed of softer clayey soils exhibit more intense amplification behavior at eastern edge. Besides, the concentration of the waves at western edge gives rise to the greater local amplification at points close to outcrop at lower frequencies. On the other hand, for basin with stiff clay, the MSAFs of the obliquely incident waves are generally greater at the basin center with respect to the vertically propagating wave case.

In addition to the above mentioned factors, the change in the PGA level affects the results. The increase in the PGA level doesn't necessarily intensify the amplification response of the whole basin. The interaction among the affecting factors may result in smaller amplification in some points because of the nonlinearity effect. Nevertheless, the increase in the motion strength increases the possibility of the nonlinear behavior in the basin. It should be noted that although the occurred nonlinearity level is not measured in this study, the application of the fully nonlinear method along with the hysteresis damping scheme ensures the consideration of the nonlinearity in the analyses. The occurrence of the nonlinearity can be traced in the presented results. For example, the shift in the period of the maximum SAF curves by the increases in the PGA level of the induced motion can be attributed to such effect. However, the explanation of the occurred nonlinearity level needs more detailed investigation, which is out of the scope of the present study.

5. Conclusions

In this study, the effect of incident angle on the dynamic response of the shallow basins was investigated. The numerical analyses of the basins filled with three different clay types were performed using a fully nonlinear method. Using the obtained results, the influences of some parameters such as basin edge, PGA level of the bedrock motion and incident angle as well as different clay types on the amplification behavior of the basin were investigated.

The results showed that despite the symmetric geometry of the basin, the change in the incident angle affects the response at two edges as well as the central part. It was seen that in soft clayey basins the effect of the 45◦ incident angle is dominant at eastern half at PGA levels of 0.2 g, 0.3 g and 0.4 g. Also, the effect of the 45◦ incident angle is dominant at central part of the medium clayey basin. At stiff clayey basin, except at the edges, the effect of 30◦ and 45◦ incident angles are dominant at other cases. Therefore, it can be concluded that the effect of the obliquely subjected waves is dominant at most cases. Also, the effect of vertically propagating waves are generally dominant at the basin edges. The higher effect of the 45◦ incident angle on the basin response can be concluded.

Since the maximum spectral amplification factor curves give no information about their corresponding period, to see the change in their corresponding period, the spectral amplification curves of the surface points were compared. It was seen that different parts of the valleys are sensitive to different periods. While the lateral parts are sensitive to lower periods, the maximum amplification of the inner parts takes place at longer periods. By the increase in the PGA level of the motions, the period of the maximum spectral amplification factor of the surface points increases. Also, it was seen that the change in the type of the clay affects the response of the basin. The greatest maximum spectral amplification factors belong to the basin with soft clayey soil.

References

Abraham J.R., Lai C.G. and Papageorgiou A. (2015), "Basin-effects observed during the 2012 Emilia earthquake sequence in Northern Italy", *Soil Dyn. Earthq. Eng.*, **78**, 230-242. https://doi.org/10.1016/j.soildyn.2015.08.007.

Aki, K. and Larner K.L. (1970), "Surface motion of a layered medium having an irregular interface due to incident plane SH waves", *J. Geophys. Res.*, **75**, 933-954.

Anbazhagan, P., Aditya, P. and Rashmi, H.N. (2011), "Amplification based on shear wave velocity for seismic zonation: comparison of empirical relations and site response results for shallow engineering bedrock sites", *Geomech. Eng.*, **3**(3), 189-206. https://doi.org/10.12989/gae.2011.3.3.189

Assimaki, D. and Gazetas, G. (2004), "Soil and topographic amplification on canyon banks and the 1999 Athens earthquake", *J. Earthq. Eng.*, **8**(1), 1-43. https://doi.org/10.1142/S1363246904001250.

Bakir, B.S., Ozkan, M.Y. and Ciliz, S. (2002), "Effects of basin edge on the distribution of damage in 1995 Dinar, Turkey earthquake", *Soil Dyn. Earthq. Eng.*, **22**, 335-345. https://doi.org/10.1016/S0267-7261(02)00015-5.

Chavez-Garcia, F.J., Raptakis, D., Makra, K. and Pitilakis, K. (2000), "Site effects at Euroseistest- II. Results from 2D numerical modeling and comparison with observations", *Soil Dyn. Earthq. Eng.*, **19**, 23-39. https://doi.org/10.1016/S0267-7261(99)00026-3.

Costanzo, A., d'Onofrio, A. and Silvestri, F. (2019), "Seismic response of a geological, historical and architectural site: the Gerace cliff (southern Italy)", *Bull. Eng. Geol. Environ.*, https://doi.org/10.1007/s10064-019-01515-0.

Cundall, P.A. *et al*. (1980), NESSI—soil structure interaction program for dynamic and static problems. Norwegian Geotechnical Institute, Report 51508-9.

Cundall, P.A. (2008), *FLAC3D Manual: a computer program for fast Lagrangian analysis of Continua (Version 4.0)*. Minneapolis, MN, USA.

Faccioli, E., Vanini, M. and Frassine, L. (2002), "Complex site effects in earthquake ground motion, including topography", *Proceedings of the 12th European conference on earthquake engineering*, Paper Reference: 844.

Gautam, D., Forte, G. and Rodrigues, H. (2016), "Site effects and associated structural damage analysis in Kathmandu Valley", *Nepal. Earthq. Struct.*, **10**(5), 1013-1032. https://doi.org/10.12989/eas.2016.10.5.1013.

Gelagoti, F., Kourkoulis, R., Anastasopoulos, I., Tazoh, T. and Gazetas, G. (2010), "Seismic wave propagation in a very soft alluvial valley: sensitivity to ground-motion details and soil nonlinearity, and generation of a parasitic vertical component", *Bull, Seismol, Soc, Am,*, **100**(6), 3035-3054. https://doi.org/10.1785/0120100002.

Gil-Zepeda, S.A., Montalvo-Arrieta, J C., Vai, R. and Sanchez-Sesma, F.J. (2003), "A hybrid indirect boundary element-discrete wave number method applied to simulate the seismic response of stratified alluvial valleys", *Soil Dyn. Earthq. Eng.*, **23**, 77-86. https://doi.org/10.1016/S0267-7261(02)00092-1.

Hasal, M.E., Iyisan, R. and Yamanaka, H. (2018), "Basin edge effect on seismic ground response: a parametric study for Duzce basin case, Turkey", *Arabian J. Sci. Eng.*, **43**(4), 2069-2081. https://doi.org/10.1007/s13369-017-2971-7.

Heymsfield, E. (2000), "Two-dimensional scattering of SH waves in a soil layer underlain with bedrock", *Soil Dyn. Earthq. Eng.*, **19**, 489-500. https://doi.org/10.1016/S0267-7261(00)00030-0.

Ishibashi, I. and Zhang, X. (1993), "Unified dynamic shear moduli and damping ratios of sand and clay. Soils and foundations", *Jap. Soc. Soil Mech. Found. Eng.*, **33**(1), 182-191. https://doi.org/10.3208/sandf1972.33.182.

Iyisan, R. and Khanbabazadeh, H. (2013), "A numerical study on the basin edge effect on soil amplification", *Bull. Earthq. Eng.*, **11**, 1305-1323. https://doi.org/10.1007/s10518-013-9451-6.

Jakka, R.S., Hussain, M.D. and Sharma, M.L. (2015), "Effects on amplification of strong ground motion due to deep soils", *Geomech. Eng.*, **8**(5), 663-674. https://doi.org/10.12989/gae.2015.8.5.663

Kamalian, M., Jafari, M.K, Sohrabi-Bidar, A., Razmkhah, A. and Gatmiri, B. (2006), "Time domain two-dimensional site response analysis of non-homogeneous topographic structures by a hybrid BE/FE method", *Soil Dyn. Earthq. Eng.*, **26**, :753-765. https://doi.org/10.1016/j.soildyn.2005.12.008.

Kamiyama, M. and Satoh, T. (2002), "Seismic response analysis of laterally inhomogeneous ground with emphasis on strains", *Soil Dyn. Earthq. Eng.*, **22**, 877-884. https://doi.org/10.1016/S0267-7261(02)00110-0

Kawase, H. and Aki, K. (1989), "A study on the response of a soft basin for incident. S, P and Rayleigh waves with special reference to the long duration observed in Mexico City", *Bull. Seismol. Soc. Am.*, **79**, 1361-1382.

Khanbabazadeh, H., Hasal, M.E. and Iyisan, R. (2019), "2D seismic response of the Duzce Basin, Turkey", *Soil Dyn. Earthq. Eng.*, **125**, 105754. https://doi.org/10.1016/j.soildyn.2019.105754.

Khanbabazadeh, H. and Iyisan, R. (2014a), "A numerical study on the 2D behavior of clayey basins", *Soil Dyn. Earthq. Eng.*, **66**, 31-41. https://doi.org/10.1016/j.soildyn.2014.06.029.

Khanbabazadeh, H. and Iyisan, R. (2014b), "A numerical study on the 2D behavior of the single and layered clayey basins", *Bull. Earthq. Eng.*, **12**, 1515-1536. https://doi.org/10.1007/s10518-014-9590-4.

Khanbabazadeh, H., Iyisan, R., Ansal, A. and Zulfikar, C. (2018), "Nonlinear dynamic behavior of the basins with 2D bedrock", *Soil Dyn. Earthq. Eng.*, **107**, 108-115, https://doi.org/10.1016/j.soildyn.2018.01.011.

Khanbabazadeh, H., Iyisan, R., Ansal, A. and Hasal, M.E. (2016), "2D non-linear seismic response of the Dinar basin,Turkey", *Soil Dyn. Earthq. Eng.*, **89**, 5-11. https://doi.org/10.1016/j.soildyn.2016.07.021.

Khanbabazadeh, H., Zulfikar, A.C. and Yesilyurt A. (2020), "Basin edge effect on industrial structures damage pattern at clayeybasins",*Geomech. Eng.*, **23**(6), 575-585. https://doi.org/10.12989/gae.2020.23.6.575.

Kham, M., Semblat, J.F. and Bouden-Romdhane, N. (2013), "Amplification of seismic ground motion in the Tunis basin: numerical BEM simulations vs. experimental evidence", *Eng. Geol.*, **154**, 80-86. https://doi.org/10.1016/j.enggeo.2012.12.016.

Kuhlemeyer, R.L. and Lysmer, J. (1973), "Finite element method accuracy for wave propagation problems", *J. Soil Mech. Found. Div. ASCE*, **99**(5), 421-427.

Lysmer, J. and Kuhlemeyer, R.L. (1969), "Finite dynamic model for infinite media", *J. Eng. Mech.*, **95**(4), 859-877

Makra, K., Chavez-Garcıa, F.J., Raptakis, D. and Pitilakis K. (2005), "Parametric analysis of the seismic response of a 2D sedimentary valley: implications for code implementations of complex site effects", *Soil Dyn Earthq Eng*, **25**:303–315. https://doi.org/10.1016/j.soildyn.2005.02.003

Makra, K. and Chavez-Garci, F.J. (2016), "Site effects in 3D basins using 1D and 2D models: an evaluation of the differences based on simulations of the seismic response of Euroseistest", *Bull. Earthq. Eng.*, **14**, 1177-1194. https://doi.org/10.1007/s10518-015-9862-7.

Madiai, C., Facciorusso, J., Gargini, E. and Baglione, M. (2016), "1D versus 2D site effects from numerical analyses on a cross section at Barberino di Mugello (Tuscany, Italy)", *Procedia Eng.*, **158**, 499-504. https://doi.org/10.1016/j.proeng.2016.08.479.

Manakou, M.V., Raptakis, D.G., Chavez-Garci, F.J., Apostolidis, P.I. and Pitilakis, K.D. (2010), "3D soil structure of the Mygdonian basin for site response analysis", *Soil Dyn. Earthq. Eng.*, **30**, 1198-1211. https://doi.org/10.1016/j.soildyn.2010.04.027.

Paolucci, R. (1999), "Shear resonance frequencies of alluvial

valleys by Rayleigh's method", *Earthq. Spectra*, **15**(3), 503-521. https://doi.org/10.1193/1.1586055.

Pelekis, P., Batilas, A., Pefani, E., Vlachakis, V. and Athanasopoulos, G. (2017), "Surface topography and site stratigraphy effects on the seismic response of a slope in the Achaia-Ilia (Greece) 2008 Mw6.4 earthquake", *Soil Dyn. Earthq. Eng.*, **100**, 538-554. https://doi.org/10.1016/j.soildyn.2017.05.038.

Pitilakis, K. (2004), "Site effects", *Recent advances in earthquake geotechnical engineering and microzonation, vol*. 1. Netherlands: Kluwer Academic Publishers.

Raptakis, D., Chavez-Garcia, F.J., Makra, K. and Pitilakis, K. (2000), "Site effects at Euroseistest - I: determination of the valley structure and confrontation of observations with 1D analysis", *Soil Dyn. Earthq. Eng.*, **19(**1), 1-22. https://doi.org/10.1016/S0267-7261(99)00025-1.

Rodriguez-Castellanos, A., Sanchez-Sesma, F.J., Ortiz-Aleman, C. and Orozco-del-Castillo, M. (2011), "Least square approach to simulate wave propagation in irregular profiles using the indirect boundary element method", *Soil Dyn. Earthq. Eng*., **31**, 385-390. https://doi.org/10.1016/j.soildyn.2010.09.007.

Roy, N. and Sahu, R.B. (2012), "Site specific ground motion simulation and seismic response analysis for microzonation of Kolkata", *Geomech. Eng.*, **4**(1), 1-18. https://doi.org/10.12989/gae.2012.4.1.001.

Saenz, M., Sierra, C., Vergara, J., Jaramillo, J. and Gomez, J. (2019), "Site specific analysis using topography conditioned response spectra", *Soil Dyn. Earthq. Eng*., **123**, 470-497. https://doi.org/10.1016/j.soildyn.2019.03.004.

Safak, E. (2001), "Local site effects and dynamic soil behavior", *Soil Dyn. Earthq. Eng*., **21**, 453-458. https://doi.org/10.1016/S0267-7261(01)00021-5.

Saffarian, M.A. and. Bagheripour, M.H. (2014)," Seismic response analysis of layered soils considering effect of surcharge mass using HFTD approach. Part I: basic formulation and linear HFTD", *Geomech. Eng.*, **6**(6), 517-530. https://doi.org/10.12989/gae.2014.6.6.517.

Semblat, J.F., Kham, M., Parara, E., Bard, P.Y., Pitilakis, K., Makra, K. and Raptakis, D. (2005), "Seismic wave amplification: basin geometry vs soil layering", *Soil Dyn. Earthq. Eng.*, **25**, 529-538. https://doi.org/10.1016/j.soildyn.2004.11.003.

Semblat, J.F., Duval, A.M. and Dangla, P. (2000), "Numerical analysis of seismic wave amplification in Nice (France) and comparisons with experiments", *Soil Dyn. Earthq. Eng*., **19**(5), 347-362. https://doi.org/10.1016/S0267-7261(00)00016-6.

Shani-Kadmiel, S., Tsesarsky, M., Louie, J.N. and Gvirtzman, Z. (2012), "Simulation of seismic-wave propagation through geometrically complex basins: the Dead Sea Basin", *Bul.l Seismol. Soc. Am.*, **102**(4), 1729-1739. https://doi.org/10.1785/0120110254.

Shiuly, A., Sahu, R.B. and Mandal, S. (2015), "Seismic microzonation of Kolkata", *Geomech. Eng*., **9**(2), 125-144. https://doi.org/10.12989/gae.2015.9.2.125.

Sonmezer, Y.B., Bas, S., Isik, N.S. and Akbas, S.O. (2018), "Linear and nonlinear site response analyses to determine dynamic soil properties of Kirikkale", *Geomech. Eng.*, **16**(4), 435-448. https://doi.org/10.12989/gae.2018.16.4.435.

Sonmezer, Y.B. and Celiker, M. (2020), "Determination of seismic hazard and soil response of a critical region in Turkey considering far-field and near-field earthquake effect", *Geomech. Eng.*, **20**(2), 131-146. https://doi.org/10.12989/gae.2020.20.2.131.

Stanko, D., Gulerce, Z., Markusic, S. and Salic, R. (2019), "Evaluation of the site amplification factors estimated by equivalent linear site response analysis using time series and random vibration theory based approaches", *Soil Dyn. Earthq. Eng.*, **117**, 16-29. https://doi.org/10.1016/j.soildyn.2018.11.007.

Takahiro, S. (2000), "Estimation of earthquake motion incident angle at rock site", *Proceedings of the 12th World Conference Earthquake Engineering*, New Zealand.

Yniesta, S., Brandenberg ,S.J. and Shafiee, A. (2017), "ARCS: A one dimensional nonlinear soil model for ground response analysis", *Soil Dyn. Earthq. Eng.*, **102**, 75-85. https://doi.org/10.1016/j.soildyn.2017.08.015.

You, H.B., Zhao, F.X. and Rong, M.S. (2009), "Nonlinear seismic response of horizontal layered site due to inclined wave", *Chinese J. Geotech. Eng.*, **31**(2), 234-240.

Zahradnik, J. (1995), "Simple elastic finite-difference scheme", *Bull. Seismol. Soc. Am.*, **85**, 1879-1887.

Zhang, J. and Zhao, J.X. (2009), "Response spectral amplification ratios from 1- and 2 dimensional nonlinear soil site models", *Soil Dyn. Earthq. Eng.*, **29**, 563-573. https://doi.org/10.1016/j.soildyn.2008.06.006.

Zhu, C., Chavez-Garcia, F.J., Thambiratnam, D. and Gallage, C. (2018), "Quantifying the edge-induced seismic aggravation in shallow basins relative to the 1D SH model", *Soil Dyn. Earthq. Eng*., **115**, 402-412. https://doi.org/10.1016/j.soildyn.2018.08.025.

Zhu, C. and Thambiratnam, D. (2016), "Interaction of geometry and mechanical property of trapezoidal sedimentary basins with incident SH waves", *Bull. Earthq. Eng.*, **14**, 2977-3002. https://doi.org/10.1007/s10518-016-9938-z.

Zhu, C., Thambiratnam, D. and Zhang J. (2015), "Seismic Response of Sedimentary Basin Subjected to Obliquely Incident SH Waves", *Proceedings of the 6th International Conference on Earthquake Geotechnical Engineering*, 1-4 November 2015 Christchurch, New Zealand.

GC